Large-Scale Atmospheric Mixing As Deduced from the Seasonal and Meridional Variations of Carbon Dioxide

B. BOLIN AND C. D. KEELING[1]

International Meteorological Institute, Stockholm, Sweden

Abstract. Representative data on the variations of carbon dioxide in the atmosphere are presented. The data reveal a presumably natural source in the tropical oceanic areas and the industrial source of midlatitudes. Using a simple model of large-scale exchange, the meridional eddy exchange coefficient is computed to be about 3×10^{10} cm^2 sec^{-1}, and the meridional transport from tropical to north polar areas is computed to be about 2×10^{10} metric tons of carbon dioxide per year. An analysis of the seasonal variation shows that land vegetation north of 45°N is responsible for a net consumption of carbon dioxide of about 1.5×10^{10} tons during the vegetation period in summer. It is concluded that carbon dioxide is an excellent tracer for the study of atmospheric mixing processes. More data are needed, however, to make full use of it.

Introduction. Atmospheric CO_2 offers one of the most promising tracer constituents for elucidating atmospheric mixing processes on a global scale. The observed systematic variations of the content of CO_2 in the atmosphere with season, latitude, and altitude are the results of sources and sinks which exist only at the surface of the earth and which induce regular variations in the lowest layers of the atmosphere, the penetration of which upward and horizontally can yield quantitative information about the transfer mechanism of the atmosphere.

This information can be precise because CO_2 above the earth's surface is a conservative property of the air, unchanged by temperature or rainfall variations. Although representative sampling of the atmosphere is not a simple problem, the variations of CO_2 in the free atmosphere proceed with a scale of weeks and hundreds of kilometers, so that even with very limited data the essential features of the variation with space and time can be established. One can hope with a continued sampling program, still within the scope of present resources, to improve the information greatly within a few years. The sampling and analysis techniques for atmospheric CO_2 have been made sufficiently reliable to permit the ready detection of concentration differences of a few per cent of the total observed variation, in spite of the high risk of contamination.

We shall discuss data obtained during 5 years (1957–1962) from pole to pole, primarily over the Pacific Ocean. The data are published in part [*Keeling*, 1960]; publication of the remainder is in progress.

From these data we will (1) give an over-all picture of the large-scale transfer processes in the troposphere and information on the main features of sources and sinks of CO_2; (2) establish how sensitive our conclusions are to the uncertainty of the data; (3) indicate to what extent the present data are inadequate and what additional data seem necessary in order to interpret the complex motions of the atmosphere with regard to transfer processes.

The last two results are not the least important and, indeed, are of interest when we are considering any tracer constituent in the atmosphere.

Analysis of data. The data establish the major features of the variation with latitude and season over the Pacific Ocean from pole to pole. Only the winter months in the middle latitudes of the southern hemisphere are totally without representation. In northern latitudes the data represent as much as half the atmospheric column.

Two kinds of measurements, as reported by *Keeling* [1960], have been made. Continuously recording infrared gas analyzers have been operated at fixed stations at Point Barrow,

[1] Now at Scripps Institution of Oceanography, La Jolla, California.

Alaska, Mauna Loa Observatory, Hawaii, Little America, Antarctica, and at the south pole and on research vessels of the Scripps Institution of Oceanography. Also, over the entire region of the study, individual samples have been collected in glass flasks and analyzed in the laboratory with a gas analyzer. The location of stations and approximate positions for flask samples are shown in Figure 1. The coverage of the data is indicated in more detail in Table 1.

Wherever measurements exist for different years, an annual average concentration rise has been found. The rate of rise can be established best from the nearly continuous record of concentration at Mauna Loa Observatory, Hawaii, for the extended period, November 1958 to April

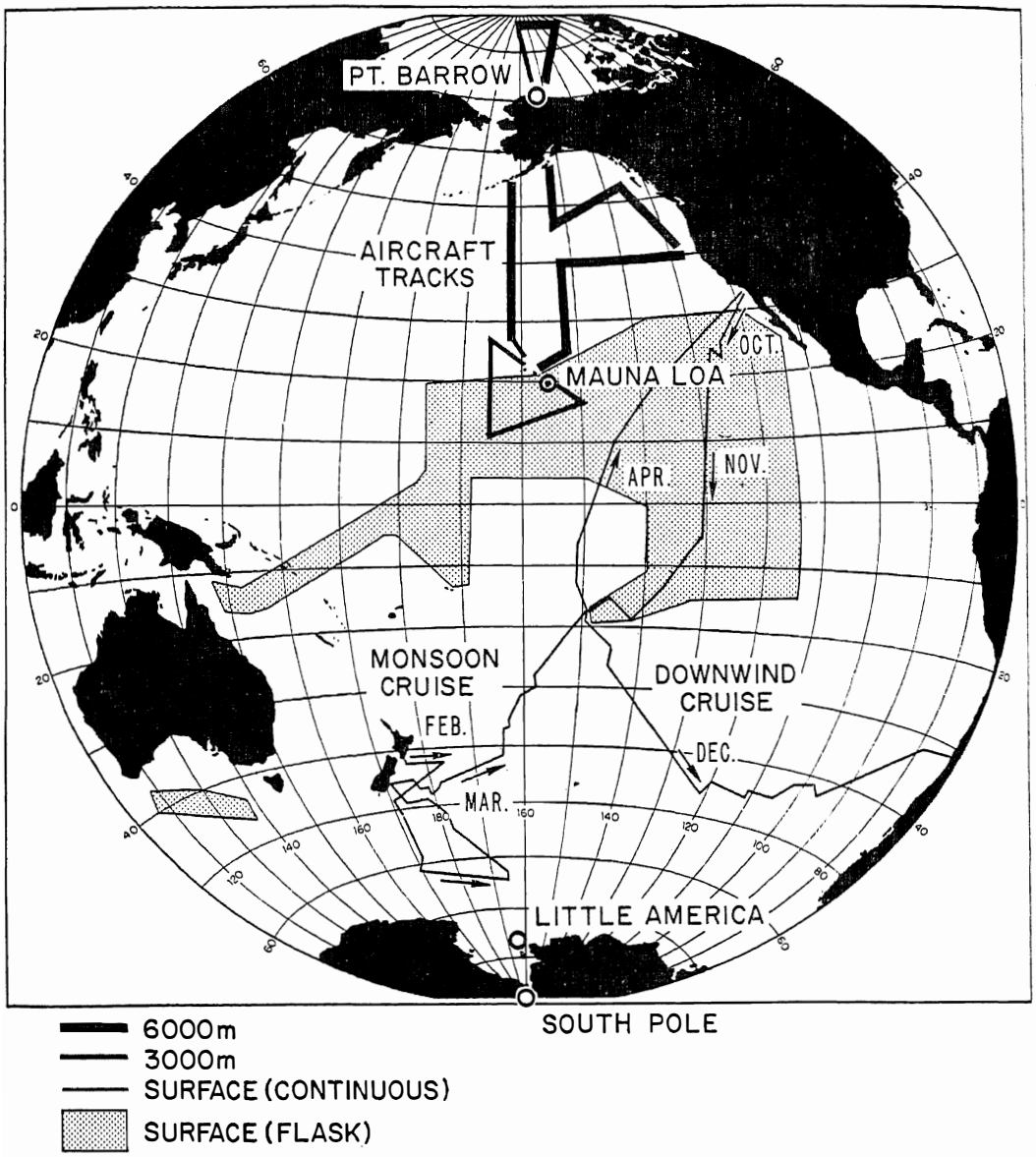

Fig. 1. Location of stations and tracks for sampling atmospheric CO_2. Location for surface flask sampling, except Downwind and Monsoon cruises, is highly generalized. Indian Ocean is not shown.

TABLE 1. Survey of Collected Data

Name	Location	Latitude	Elevation	Period of Sampling	Data
		Continuous Stations			
Point Barrow	Alaska	71°N	2 m	July 1961 to July 1962	13 months
Mauna Loa	Hawaii	19°N	3500 m	Mar. 1958 to Mar. 1962	42 months*
Little America†	Antarctica	79°S	10 m	Feb. 1958 to Oct. 1958	9 months
South Pole	Antarctica	90°S	3000 m	June 1960 to Apr. 1962	17 months‡
		Continuous Ship Sampling			
Downwind Cruise	Pacific Ocean	30°N–50°S	0–10 m	Oct. 1957 to Dec. 1957	1140 hours
Monsoon Cruise	Pacific Ocean	30°N–65°S	0–10 m	Feb. 1961 to Apr. 1961	1580 hours
		Flask Sampling by Aircraft			
Ptarmigan Flight	Arctic Ocean	86°N–70°N	500 mb	Sept. 1958 to Nov. 1961	151 flasks (21 flights)
Ptarmigan Flight	Arctic Ocean	86°N–70°N	700 mb	Aug. 1959 to Nov. 1961	76 flasks (17 flights)
Stork Flight	N. Pacific Ocean	60°N–40°N	500 mb	June 1958 to June 1961	328 flasks (30 flights)
Lark Flight	N. Pacific Ocean	40°N–20°N	500 mb	Dec. 1958 to Dec. 1961	207 flasks (20 flights)
Loon Flight	N. Pacific Ocean	30°N–10°N	700 mb	Apr. 1960 to Feb. 1961	85 flasks (7 flights)
		Flask Sampling at Stations			
Hilo	Hawaii	19°N	0–10 m	Mar. 1960 to July 1962	75 flasks
		Flask Sampling from Ships			
Downwind Cruise§	Pacific Ocean	30°N–50°S	0–10 m	Oct. 1957 to Dec. 1957	12 flasks
Limbo Cruise	Pacific Ocean	30°N–20°N	0–10 m	May 1960 to June 1960	32 flasks
Tethys Cruise	Pacific Ocean	30°N–5°S	0–10 m	June 1960 to July 1960	42 flasks
Monsoon Cruise	Pacific & Indian oceans	30°N–50°S	0–10 m	Aug. 1960 to Jan. 1961	51 flasks
Monsoon Cruise§	Pacific Ocean	30°N–65°S	0–10 m	Feb. 1961 to Apr. 1961	74 flasks
Risepac Cruise	Pacific Ocean	25°N–20°S	0–10 m	Oct. 1961 to Jan. 1962	36 flasks
Hilo Cruise	Pacific Ocean	30°N–20°N	0–10 m	Mar. 1962 to May 1962	18 flasks
Proa Cruise	Pacific Ocean	20°N–10°S	0–10 m	Aug. 1962	24 flasks
Total number of flasks					1223

* June and October 1958 missing.
† In the figures these data are combined with the data for the south pole.
‡ September 1960 to February 1961 missing.
§ In the figures these data are combined with continuous shipboard sampling data.

1962. From a plot of the average concentration for successive 12-month intervals (Figure 2) the rate is found to be approximately 0.06 ppm per month. This value has been used to adjust all of the measured values to a datum of January 1960. The adjusted data from different years have then been combined to construct average variations with season, latitude, and altitude.

The data are too numerous to tabulate here, but the average values of concentration at each altitude have been plotted versus latitude for each month (Figures 3 to 14). Similar graphs of concentration versus time were prepared for each latitude belt. Several, but not all, of these seasonal graphs are shown in Figures 15 to 18.

In the actual preparation the data were first sorted into the latitude intervals indicated in Table 2 and then plotted with respect to the proper calendar month. Smoothed curves were drawn with respect to both latitude and season with the constraint that the two modes of plotting be consistent. Using these smoothed curves to approximate the expected variations with latitude and season, we corrected the data to apply to the fifteenth of the month in question and to a specific plotting latitude within

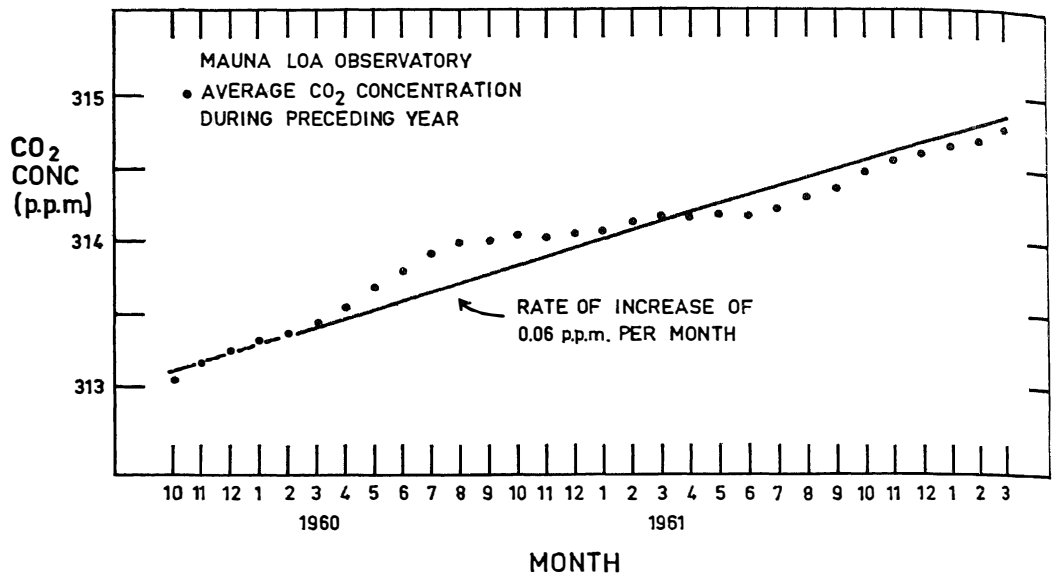

Fig. 2. Annual average concentration of CO_2 at Mauna Loa Observatory, Hawaii.

each latitude belt (see Table 2). The adjustment had very little effect except for the summer months in the northern hemisphere, where such strong gradients exist that the difference of a few days or degrees is significant. Poleward from 40°N no latitude adjustment was required since the data for each belt were always collected at the same average latitude. The data here, therefore, from the beginning, could be plotted in final form for each belt with due

TABLE 2. Scheme for Sorting Data into Latitude Intervals

Latitude Interval	Plotting Latitude	Data Used		
		500 mb	700 mb	Surface
86–70°N	78.0°N	Ptarmigan	Ptarmigan	
	71.0°N			Point Barrow
60–40°N	50.0°N	Stork		
41–35°N	40.0°N	Lark		
35–30°N	32.5°N	Lark		
30–25°N	27.5°N	Lark	Loon	Ship
25–20°N	22.5°N	Lark	Loon	Ship
	19.0°N			Mauna Loa
	19.0°N			Hilo
20–15°N	17.5°N		Loon	Ship
15–10°N	12.5°N		Loon	Ship
10– 5°N	7.5°N			Ship
5– 0°N	2.5°N			Ship
0– 5°S	2.5°S			Ship
5–10°S	7.5°S			Ship
10–15°S	12.5S°			Ship
15–20°S	17.5°S			Ship
20–40°S	30.0°S			Ship
40–65°S	50.0°S			Ship
	90.0°S			South Pole

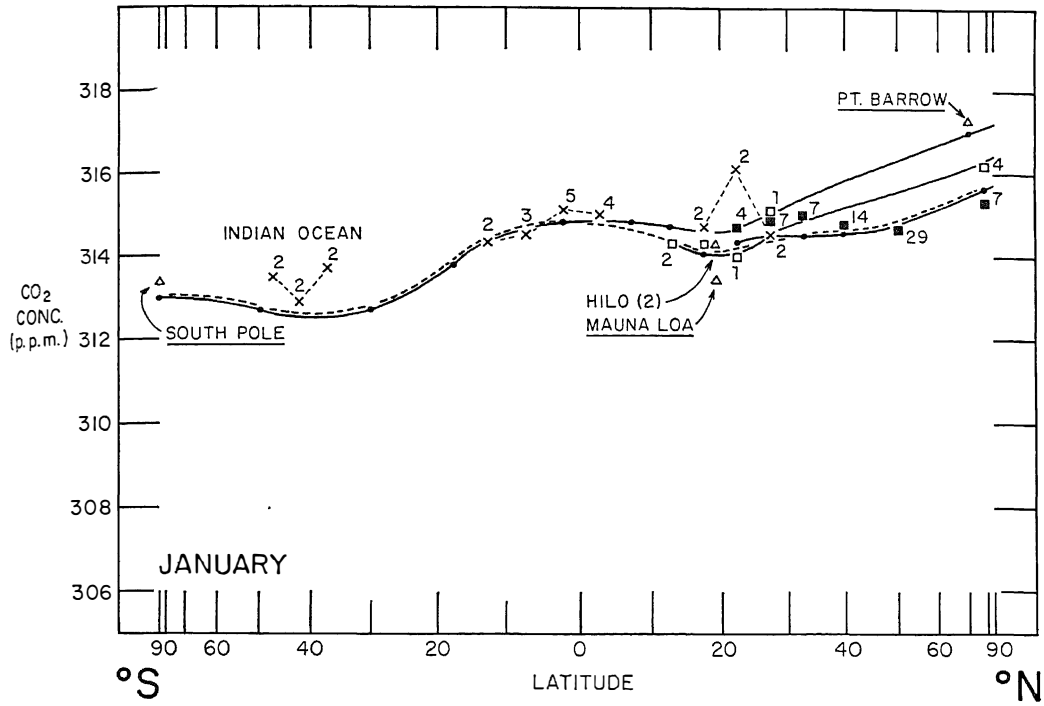

Figs. 3–14. The concentration of atmospheric CO_2 at the surface, at 700 mb, and at 500 mb from the north pole to the south pole at approximately 150°W for each calendar month. Direct data are shown as follows: continuous stations and Hilo by triangles, aircraft 500 mb by solid square, aircraft 700 mb by open square, shipboard continuous and flask sampling by x. Data obtained from continuous gas analyzers are indicated by underlining the name. Data obtained from flasks are noted by numbers appearing near each symbol. These specify the number of flasks contributing to the average value plotted. Data from the Indian Ocean are specifically designated. Smoothed values at separate levels are shown by solid circles plotted at each latitude for which a seasonal plot was constructed. Circles are connected together by solid curved lines, except that such a circle is omitted if it would fall within 0.1 ppm of a direct data symbol. The composite curves corresponding to the data of Table 3 are shown by heavy dashed lines extending from pole to pole. Light-weight straight dashed lines connect direct data belonging to a single group.

regard for the actual date of sampling. At other latitudes the adjusted data were replotted and new smoothed curves obtained.

In the interval 15° to 20°N the 700-mb seasonal curve was drawn to agree approximately with both the aircraft data and the data for the Mauna Loa Observatory and Hilo (Figure 18). From October to May, months in which the aircraft data are too sparse to permit us to make a reliable judgment of the trend, the nearly linear rate of rise observed at Mauna Loa has been assumed to apply. From May to October, on the other hand, Mauna Loa data show a sharper decline in concentration than is seen in any aircraft data from the equator to as far north as 30°N. For these months the smoothed curves were drawn in favor of the aircraft data as shown in Figure 17, and they depart considerably from the plot of the Mauna Loa data. Furthermore, the Mauna Loa data are on the average about 0.8 ppm lower than the smoothed curve for 700 mb (Figure 18). This unexpected result suggests a systematic error between measurements by flask and by continuous analyzer. Such an error is largely discounted, however, because flasks exposed at the observatory over a period of 2 years agree with the analyzer to within 0.3 ppm. A similar agreement is found in comparing the results from the analyzer with samples collected the same day by aircraft near the Hawaiian Islands. If two sampling periods are excluded because of

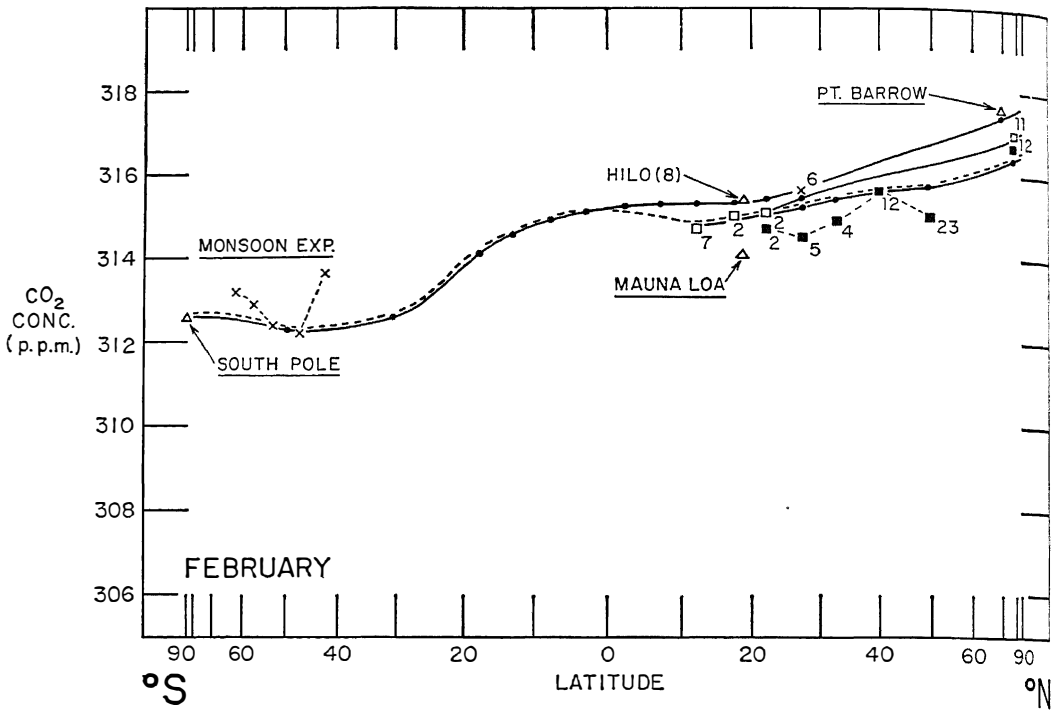
318
316
314
312
310
308
306
CO_2 CONC. (p.p.m.)
PT. BARROW
HILO (8)
MONSOON EXP.
MAUNA LOA
SOUTH POLE
FEBRUARY
90 60 40 20 0 20 40 60 90
°S
LATITUDE
°N

Fig. 4

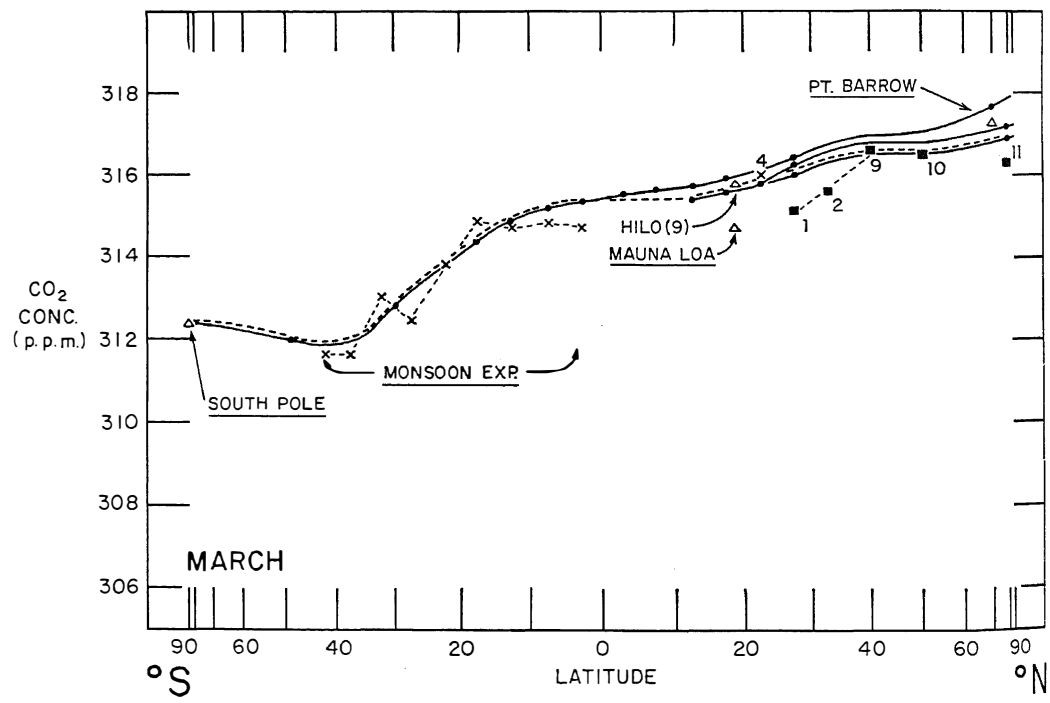
318
316
314
312
310
308
306
CO_2 CONC. (p.p.m.)
PT. BARROW
HILO (9)
MAUNA LOA
MONSOON EXP.
SOUTH POLE
MARCH
90 60 40 20 0 20 40 60 90
°S
LATITUDE
°N

Fig. 5

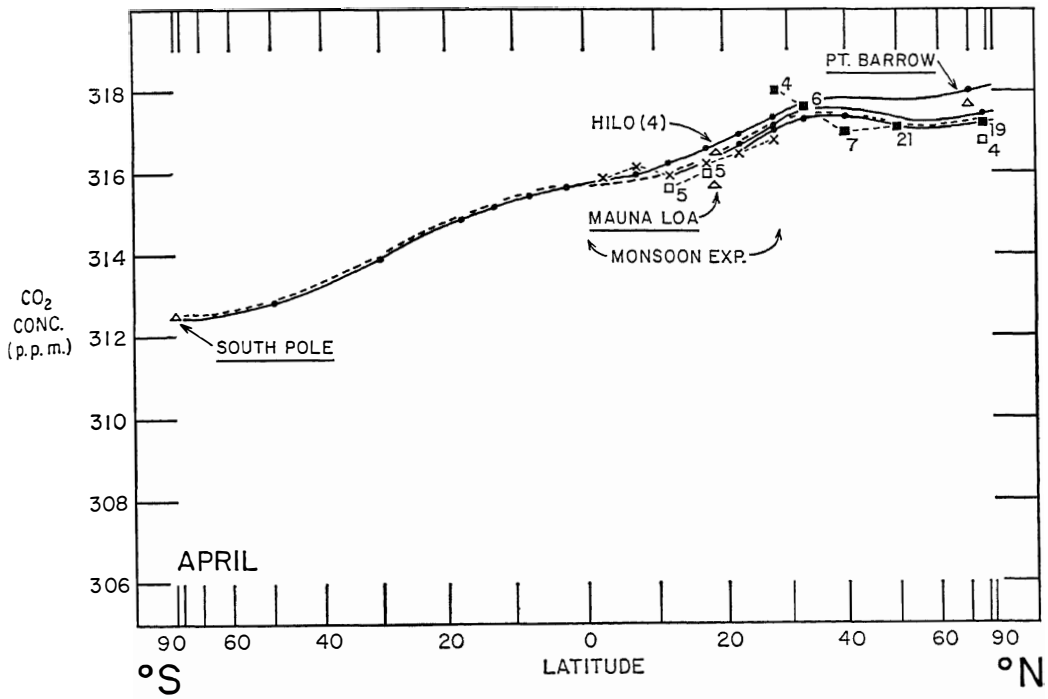
PT. BARROW
HILO (4)
MAUNA LOA
MONSOON EXP.
SOUTH POLE
APRIL
CO_2 CONC. (p.p.m.)
318
316
314
312
310
308
306
90 60 40 20 0 20 40 60 90
°S
LATITUDE
°N

Fig. 6

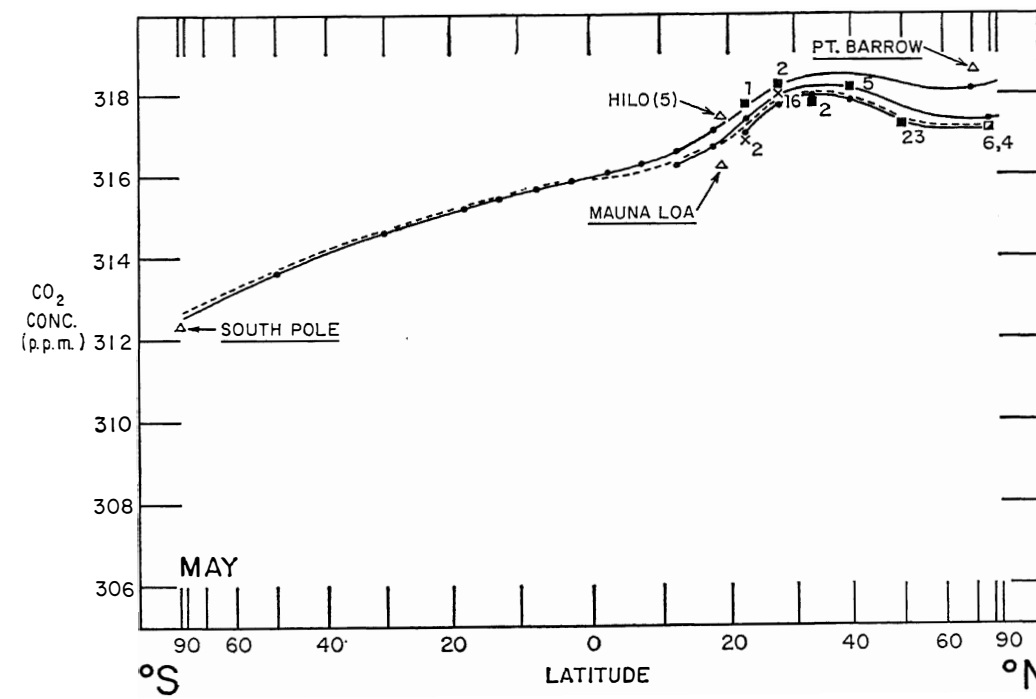
PT. BARROW
HILO (5)
MAUNA LOA
SOUTH POLE
MAY
CO_2 CONC. (p.p.m.)
318
316
314
312
310
308
306
90 60 40 20 0 20 40 60 90
°S
LATITUDE
°N

Fig. 7

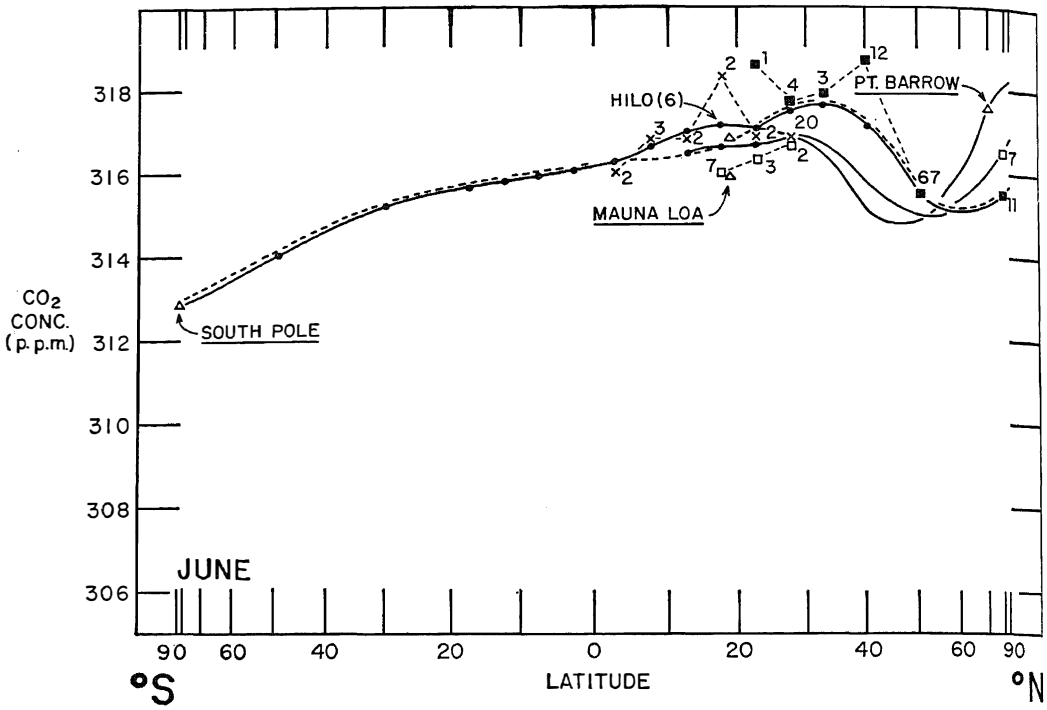
318
316
314
312
310
308
306
CO2 CONC. (p.p.m.)
HILO (6)
PT. BARROW
MAUNA LOA
SOUTH POLE
JUNE
90 60 40 20 0 20 40 60 90
°S
LATITUDE
°N

Fig. 8

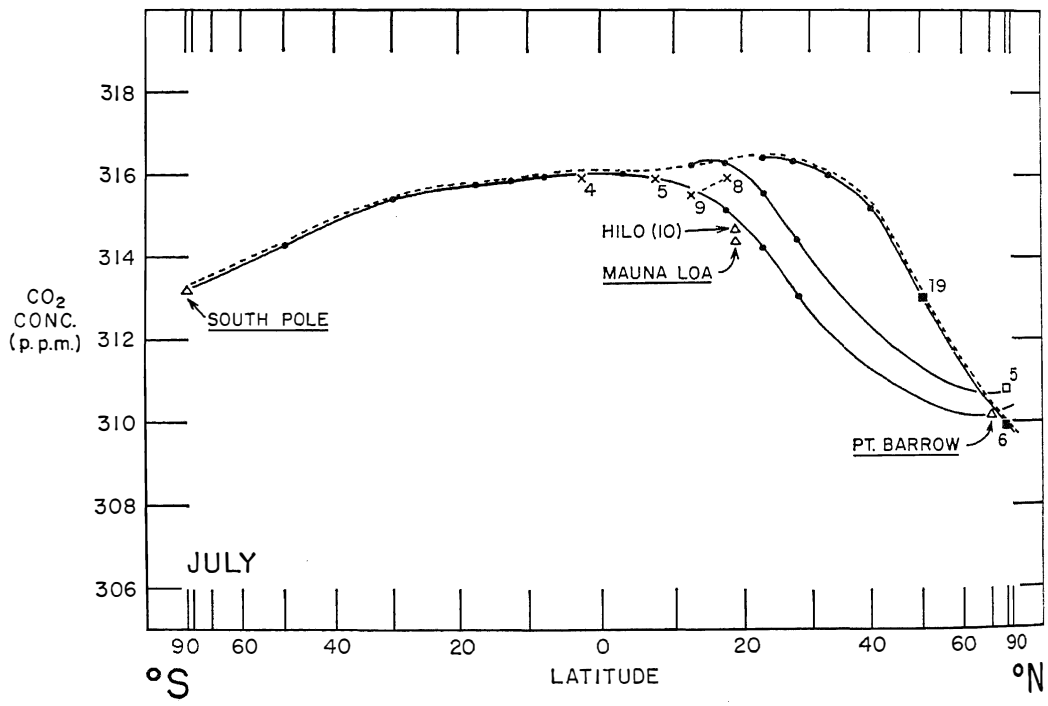
318
316
314
312
310
308
306
CO2 CONC. (p.p.m.)
HILO (10)
MAUNA LOA
SOUTH POLE
PT. BARROW
JULY
90 60 40 20 0 20 40 60 90
°S
LATITUDE
°N

Fig. 9

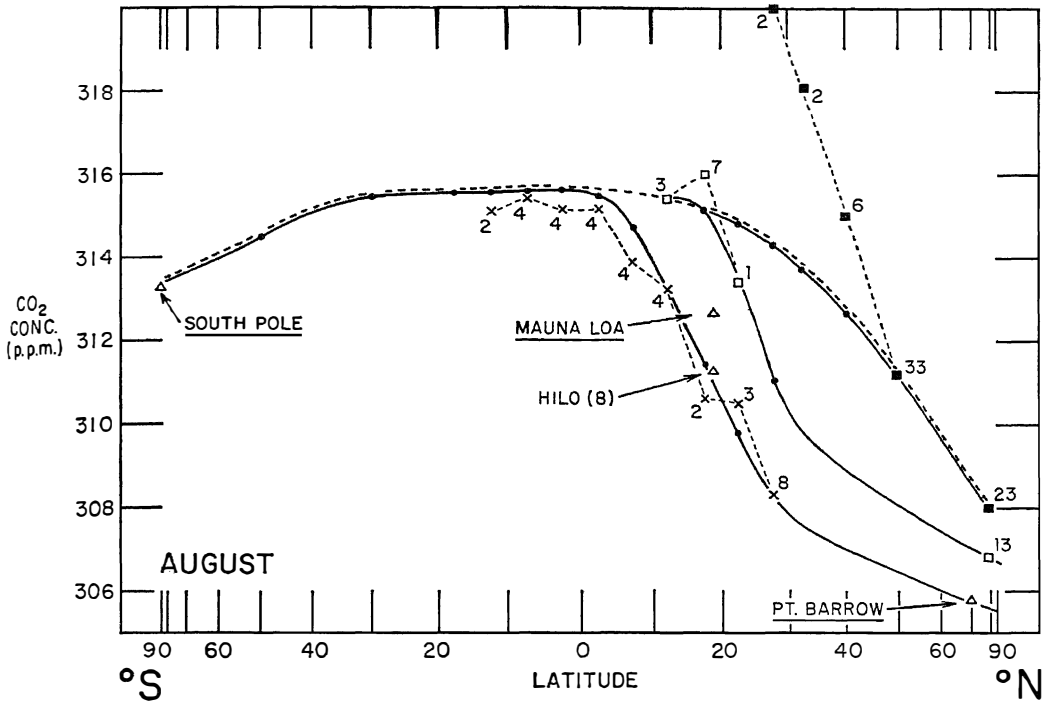
318
316
314
312
310
308
306
CO_2 CONC. (p.p.m.)
SOUTH POLE
MAUNA LOA
HILO (8)
PT. BARROW
AUGUST
90 60 40 20 0 20 40 60 90
°S
LATITUDE
°N

Fig. 10

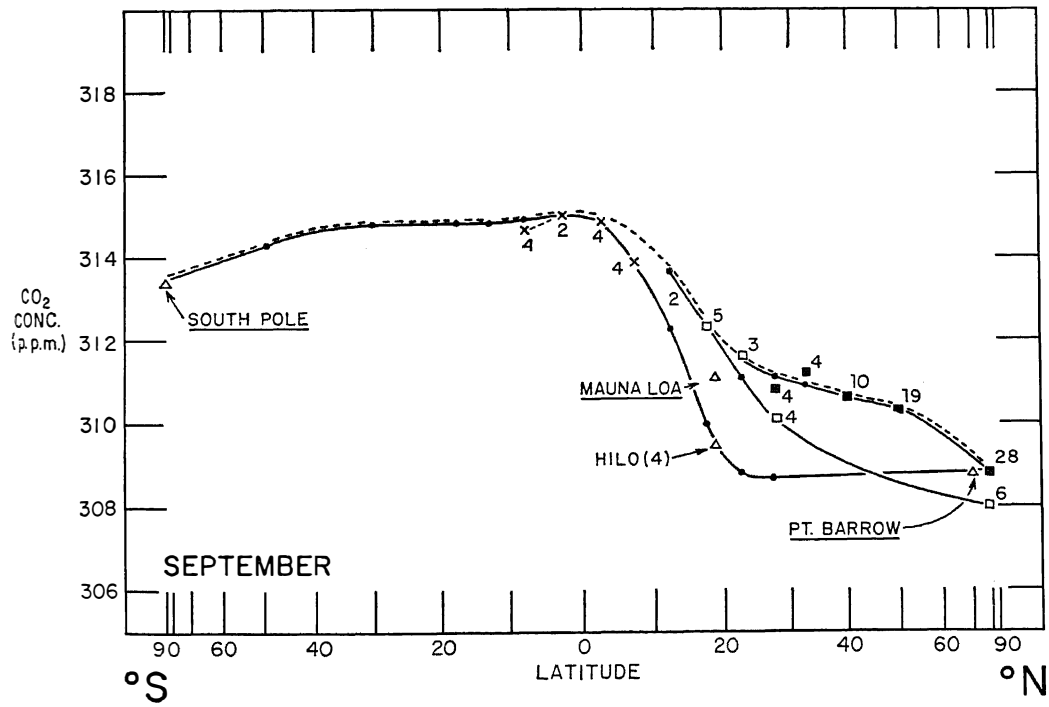
318
316
314
312
310
308
306
CO_2 CONC. (p.p.m.)
SOUTH POLE
MAUNA LOA
HILO (4)
PT. BARROW
SEPTEMBER
90 60 40 20 0 20 40 60 90
°S
LATITUDE
°N

Fig. 11

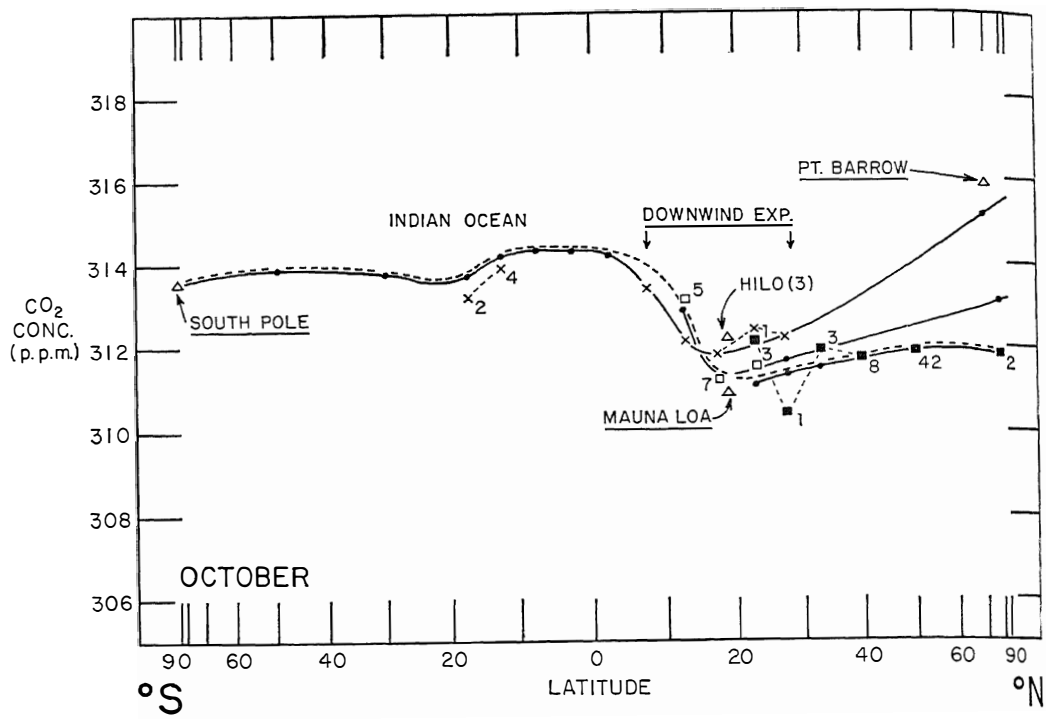
318
316
314
312
310
308
306
CO_2 CONC. (p.p.m.)
PT. BARROW
INDIAN OCEAN
DOWNWIND EXP.
HILO (3)
SOUTH POLE
MAUNA LOA
OCTOBER
90 60 40 20 0 20 40 60 90
°S
LATITUDE
°N

Fig. 12

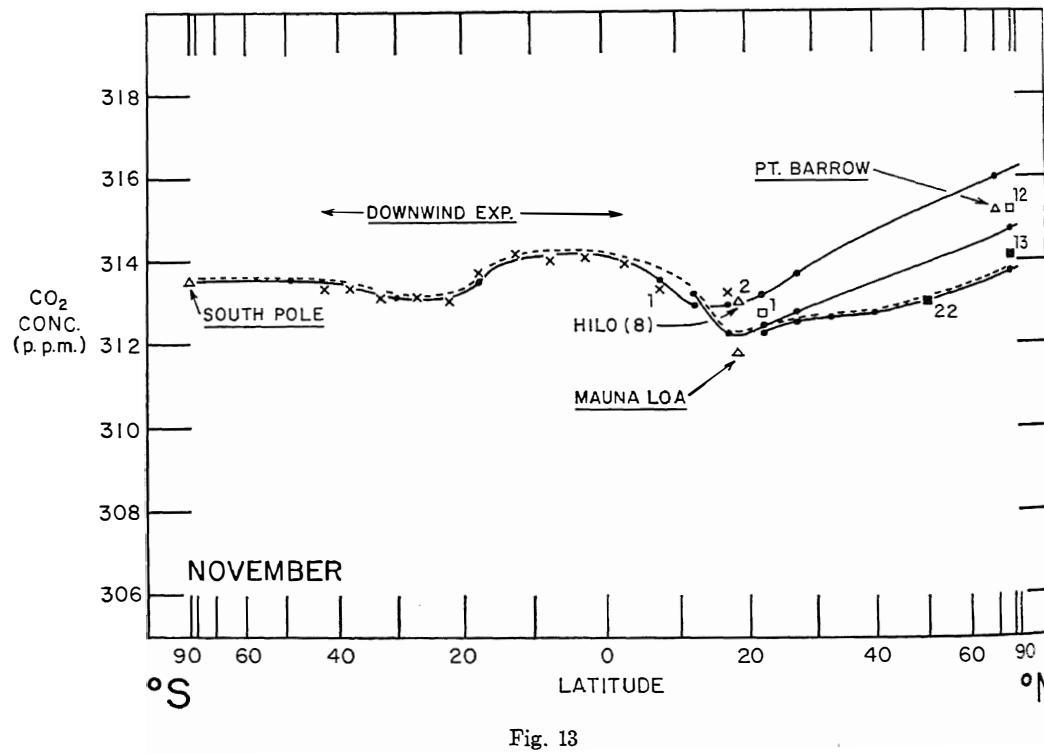
318
316
314
312
310
308
306
CO_2 CONC. (p.p.m.)
PT. BARROW
DOWNWIND EXP.
SOUTH POLE
HILO (8)
MAUNA LOA
NOVEMBER
90 60 40 20 0 20 40 60 90
°S
LATITUDE
°N

Fig. 13

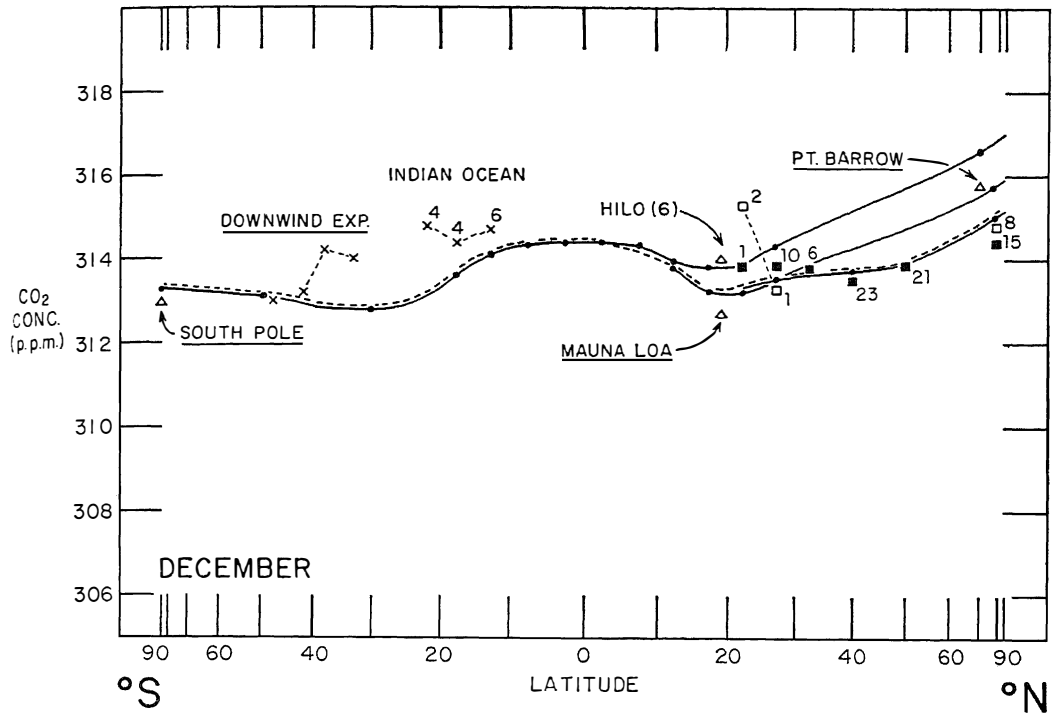

Fig. 14

special circumstances, the aircraft data agree with the analyzer to within 0.2 ppm [*Pales and Keeling*, 1963]. Taking into account all available evidence, we are unable to establish any single principal cause of the discrepancy, but have concluded that (1) contamination of the aircraft samples, (2) systematic variations between methods, and (3) lowering of CO_2 concentrations at Mauna Loa by vegetation on Hawaii each may have contributed to the total error.

At the south pole and at Point Barrow no such discrepancy has been found, but these results are based only on a preliminary evaluation of the data. Thus, for the present, even for these stations we cannot rule out the possibility of discrepancies as high as 1.0 ppm.

In the southern hemisphere seasonal plots could be constructed reliably only from 0° to 5°S, and near the south pole. To complete the seasonal representation at other latitudes the annual average concentration was assumed to be symmetrical about the equator from 20°N to 20°S (dashed curve in Figure 20), while farther south a nearly linear interpolation of the annual average was applied to connect 20°S with the south pole. On the basis of these values and direct observations during the summer months from the equator to 65°S, the entire seasonal variation in the southern hemisphere was constructed on the assumption that the shape of the curve of the seasonal variation must be approximately as observed at the south pole and at the equator.

Establishing a latitudinal profile from pole to pole is hampered because no one elevation is represented at all latitudes. From 90°N to 30°N only the data for 500 mb give adequate coverage; from the equator to the south pole there exist only data for surface air. In the zone between the equator and 30°N, where data for several levels were available, the 700-mb level was chosen for the interval 10° to 20°N, and connecting curves were then drawn to the surface curve near 2.5°N and to the 500-mb curve near 27.5°N. The final composite curves employing 500-mb data north of 27.5°N and surface data south of 2.5°N are indicated by dashed lines in Figures 3 to 14.

Values of these composite curves at the plotting latitudes are quoted in Table 3. The dashed curves are replotted in Figure 19 for in-

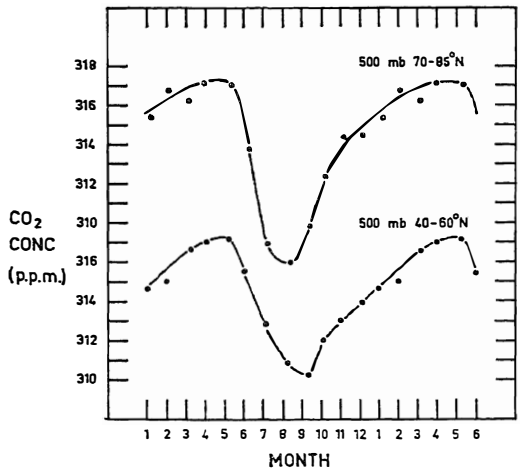

Figs. 15–18. The concentration of atmospheric CO_2 at various altitudes and latitudes as a function of the month of the year. January through June (months 1 to 6) are plotted twice to reveal the seasonal pattern more fully. Solid and open circles denote direct data. Solid curves denote values consistent with Figures 3 to 14.

tercomparison. Yearly averages of the smoothed values at each altitude and latitude are shown in Figure 20. The smoothed data suggest a net release of CO_2 near the equator, compensated for by absorption at higher latitudes, plus a source of CO_2 at 500 mb in middle latitudes of the northern hemisphere. The latter source is readily identified with the combustion of fossil fuels which causes an injection of CO_2 over the continents and should produce, on the average,

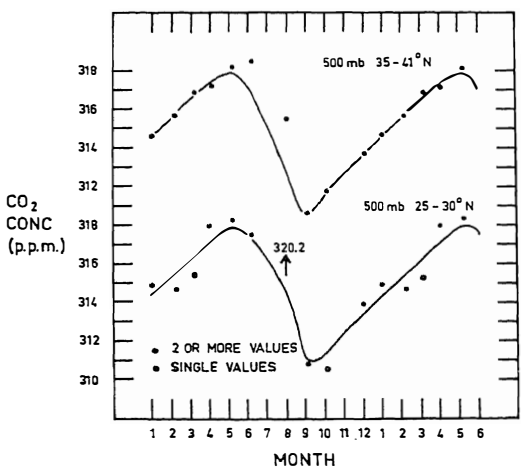

Fig. 16

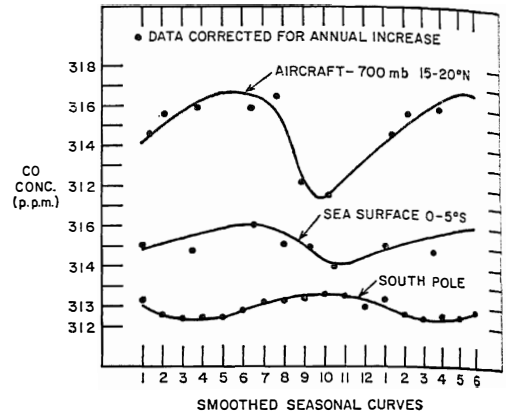

Fig. 17

a negative vertical gradient in CO_2 over the oceans, as observed. The peak near the equator must presumably be a result of a natural release of CO_2 at the ocean surface.

A model of large-scale exchange. The curves shown in Figures 19 and 20 immediately permit us to come to some qualitative conclusions regarding the distribution of sources and sinks. It is of considerable interest, however, to make quantitative estimates, which also will yield information about the intensity of the large-scale meridional mixing in the atmosphere. For the first time we have sufficient data on the distribution of a tracer gas in the atmosphere to justify a more detailed theoretical study. Still, as later discussion will demonstrate, it is important not to choose too complicated a model of the atmosphere if we are to obtain reasonable results.

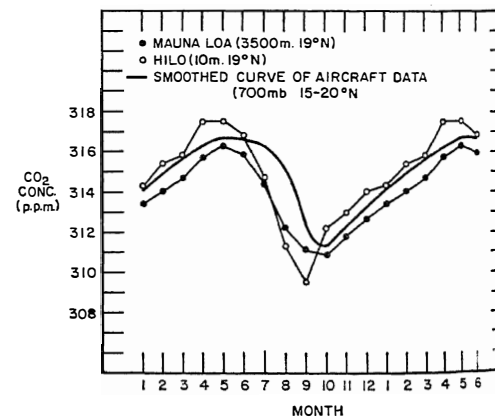

Fig. 18

TABLE 3. Smoothed Average Values of the CO_2 Concentration (in ppm) by Latitude and Month

	Jan.	Feb.	March	April	May	June	July	Aug.	Sept.	Oct.	Nov.	Dec.	Average
78.0°N	315.7	316.4	316.9	317.2	317.2	315.5	309.9	308.0	308.8	311.8	313.7	315.0	313.85
50.0°N	314.8	315.7	316.5	317.1	317.3	315.5	313.0	311.2	310.3	311.9	313.0	313.9	314.2
40.0°N	314.6	315.6	316.5	317.3	317.9	317.1	315.2	312.6	310.6	311.7	312.7	313.7	314.6
32.5°N	314.5	315.4	316.3	317.3	318.0	317.6	316.0	313.7	310.9	311.5	312.6	315.6	314.8
27.5°N	314.4	315.3	316.1	317.1	317.9	317.5	316.3	314.3	311.1	311.4	312.5	313.5	314.8
22.5°N	314.2	315.1	315.9	316.6	317.2	317.0	316.4	314.8	311.5	311.3	312.3	313.3	314.65
17.5°N	314.1	314.9	315.6	316.2	316.7	316.6	316.3	315.1	312.3	311.3	312.2	313.2	314.55
12.5°N	314.3	314.8	315.4	315.9	316.3	316.4	316.2	315.4	313.7	312.9	313.2	313.8	314.85
7.5°N	314.6	315.0	315.4	315.8	316.1	316.3	316.1	315.5	314.5	313.9	313.8	314.2	315.1
2.5°N	314.8	315.1	315.4	315.7	316.0	316.2	316.0	315.6	315.0	314.3	314.0	314.4	315.2
2.5°S	314.8	315.1	315.35	315.6	315.85	316.05	316.0	315.6	315.0	314.3	314.1	314.4	315.2
7.5°S	314.6	314.9	315.15	315.4	315.65	315.9	315.9	315.6	314.9	314.3	314.1	314.3	315.05
12.5°S	314.3	314.6	314.85	315.1	315.4	315.7	315.8	315.55	314.8	314.2	314.0	314.1	314.85
17.5°S	313.8	314.1	314.4	314.8	315.2	315.6	315.7	315.5	314.8	313.7	313.5	313.6	314.55
30.0°S	312.7	312.6	312.8	313.9	314.7	315.2	315.4	315.4	314.8	313.8	313.1	312.8	313.95
50.0°S	312.7	312.3	312.0	312.8	313.6	314.0	314.3	314.5	314.3	313.9	313.5	313.1	313.4
90.0°S	313.0	312.6	312.4	312.4	312.5	312.8	313.2	313.4	313.5	313.6	313.5	313.3	313.0

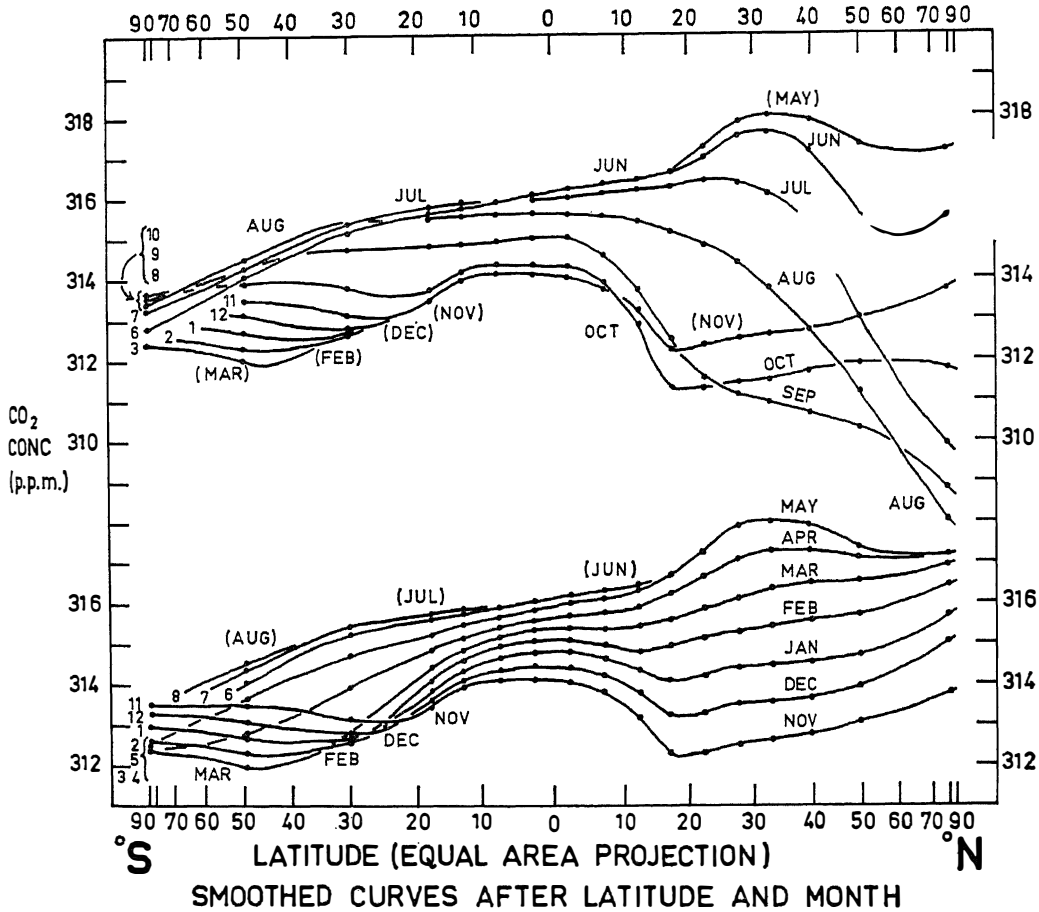

Fig. 19. Smoothed curves of the concentration of atmospheric CO_2 as a function of latitude for each calendar month. Solid circles correspond to data in Table 3.

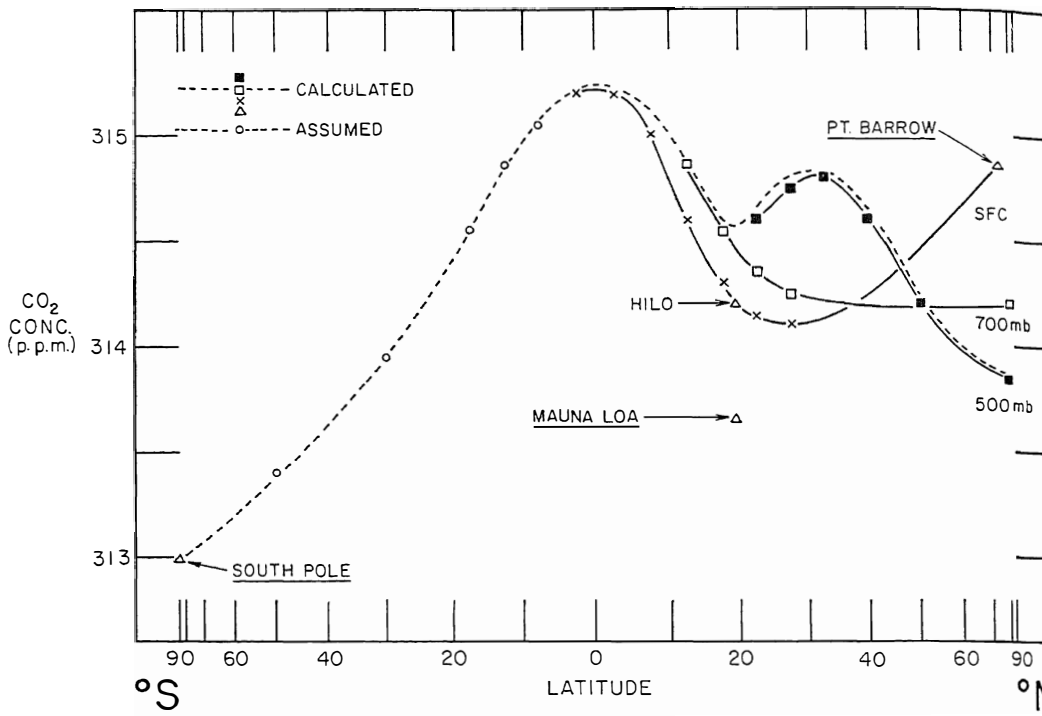

Fig. 20. Annual average concentration of atmospheric CO_2 as a function of latitude at the surface, at 700 mb, and at 500 mb, shown by the symbols x, open square, and solid square, respectively. Plotted points from 5° to 85°S (shown by open circles) are assumed values.

Only the vertically averaged CO_2 concentration in the troposphere as a function of latitude and season over the Pacific Ocean is known. In some parts, particularly middle latitudes in the southern hemisphere, even this average value is not very well known. In north polar regions, on the other hand, observations from several levels reveal a change of the direction of the vertical flux from summer to winter. It is not known how well the data actually represent the latitude belts as a whole, but this will be assumed for the moment. Some comments on this question will be given after the following analysis has been presented. Initially we shall attempt to deal only with the large-scale *meridional* exchange of CO_2.

The intensity of north-south mixing varies with latitude, and in tropical regions the Hadley meridional circulation cell also affects the rate of meridional exchange. In this study, however, we shall simply assume that the large-scale meridional exchange of CO_2 can be described by an exchange coefficient K which is independent of latitude. Denoting the CO_2 concentration by q and the CO_2 sources and sinks by $Q(\mu, t)$, where $\mu = \sin \varphi$, φ being the latitude, we may describe the changes of q in time and space by the following equation:

$$\frac{\partial q}{\partial t} = \frac{K}{a^2} \frac{\partial}{\partial \mu} \left[(1 - \mu^2) \frac{\partial q}{\partial \mu} \right] + Q(\mu, t) \qquad (1)$$

(a being the radius of the earth). The data indicate that there is a steady rise of CO_2 in the atmosphere which must be largely due to the release of CO_2 by fossil fuel combustion. The total yearly output currently amounts to approximately 1.6 ppm per year if evenly distributed over the whole earth. Part of this CO_2 goes into the oceans, probably between 50 and 60 per cent. We do not know how this sink is distributed as a function of latitude, but because of the slow rate transfer of CO_2 into the oceans the sink must be considerably more spread out than the source, which certainly has a peak in the middle latitudes in the northern hemisphere. Lacking more precise information, we shall assume that the sink is evenly distributed over the whole earth. We denote the

natural sources and sinks that exist independently of industrial contamination of the atmosphere by $Q^*(\mu)$ and the industrial source by $Q^{**}(\mu)$. Q' is the average increase of CO_2 in the atmosphere and $\hat{Q}$ is the sink of industrial CO_2, both assumed to be independent of latitude. Averaging (1) in time we thus get

$$\frac{K}{a^2}\frac{\partial}{\partial\mu}\left[(1-\mu^2)\frac{\partial\langle q\rangle}{\partial\mu}\right] + \langle Q^*(\mu) + Q^{**}(\mu)\rangle - \langle Q' + \hat{Q}\rangle \qquad (2)$$

where the angle brackets denote time average. Expanding both $\langle q\rangle$ and $\langle Q^*(\mu) + Q^{**}(\mu)\rangle - \langle Q' + \hat{Q}\rangle$ in Legendre polynomials, we get

$$\langle q(\mu)\rangle = \sum_{n=0}^{\infty}\langle q_n\rangle P_n(\mu) \qquad (3a)$$

$$\langle Q^*(\mu) + Q^{**}(\mu)\rangle - \langle Q' + \hat{Q}\rangle = \sum_{n=0}^{\infty}\langle Q_n\rangle P_n(\mu) \qquad (3b)$$

Inserting these expressions into (2) and making use of the fact that the functions $P_n(\mu)$ satisfy the differential equation

$$\frac{\partial}{\partial\mu}\left[(1-\mu^2)\frac{\partial P_n}{\partial\mu}\right] + n(n+1)P_n = 0 \qquad (4)$$

yield the following solution for the source coefficients $\langle Q_n\rangle$ in terms of the concentration coefficients $\langle q_n\rangle$:

$$\langle Q_n\rangle = \frac{K}{a^2}n(n+1)\langle q_n\rangle \qquad (5)$$

Figure 21 shows the distribution of $\langle q\rangle$ as a function of latitude. The functions $\langle q_n\rangle$ can be determined by multiplying (3a) by $P_n(\mu)$ and integrating from pole to pole ($\mu = -1$ to $\mu = 1$). The more terms that are included in this expansion, the better the fit with observed data. The dash-dotted and dashed curves in Figure 21 show the expansions including five and ten terms, respectively. Obviously, if the observed curve were representative for the whole earth, an intense permanent sink would have to be present around latitude 15°N to maintain the minimum observed at this latitude. This minimum is at least partly a result of using 500-mb data northward and surface data southward of latitude 15°N. We shall, therefore, include only the first five terms in the expansion and accordingly shall attempt to distinguish only the large-scale differences in sources in a meridional direction, such as those associated with a flux between the two hemispheres, between the poles and the equator, and between the latitude of maximum industrial output of CO_2 and the rest of the atmosphere.

We next make the plausible assumptions that the net transfer of CO_2 from one hemisphere to the other is due to the different industrial output in the two hemispheres and that the in-

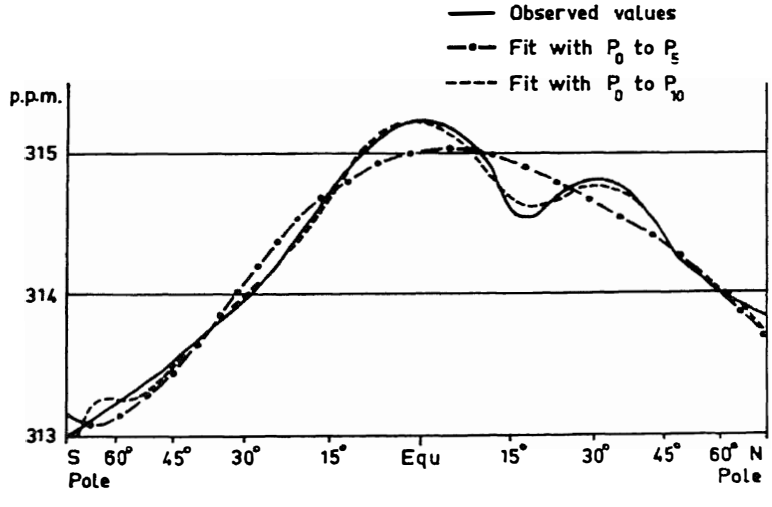

Fig. 21. The time-average concentration of CO_2, $\langle q\rangle$, as a function of latitude, compared with the fit obtained by expansion in Legendre polynomials.

dustrial sources in the southern hemisphere are negligible. The general shape of the observed curve as a function of latitude in Figure 21 immediately indicates a source in equatorial regions which presumably is a natural source. With the additional assumptions that the natural sources and sinks balance each other and also are equal in the two hemispheres, we have

$$\int_{-1}^{0} Q^*(\mu)\, d\mu = \int_{0}^{1} Q^*(\mu)\, d\mu = 0 \qquad (6)$$

and furthermore

$$\tfrac{1}{2}\int_{-1}^{1} Q^{**}(\mu)\, d\mu = Q' + \hat{Q} = 1.6 \text{ ppm} \qquad (7)$$

We can now separate the man-made and the natural sources and get

$$\begin{cases} Q^{**}(\mu) = 2\sum_{n \text{ odd}} Q_n P_n(\mu) & 0 \le \mu \le 1 \\ Q^{**}(\mu) = 0 & -1 \le \mu \le 0 \\ Q^{*}(\mu) = \sum_{n \text{ even}} Q_n P_n(\mu) & \\ \quad - \sum_{n \text{ odd}} Q_n P_n(\mu) + Q' + \hat{Q} & 0 \le \mu \le 1 \\ Q^{*}(\mu) = \sum_{n \text{ even}} Q_n P_n(\mu) & \\ \quad + \sum_{n \text{ odd}} Q_n P_n(\mu) + Q' + \hat{Q} & -1 \le \mu \le 0 \end{cases} \qquad (8)$$

With the aid of (5), (7), and (8) we can now determine K and obtain $K = 3.5 \times 10^{10}$ cm^2 sec^{-1}. This mean value for K agrees quite well with the fact that $K \approx 10^{10}$ cm^2 sec^{-1} in the surface layers of the atmosphere and may reach values of $K \approx 10^{11}$ cm^2 sec^{-1} in the upper troposphere in middle latitudes.

We can now compute both the industrial and natural sources and sinks (Figure 22). The maximum of the industrial output is found at latitude 45°N, close to 90 per cent of the total output being between latitudes 30°N and 60°N. The smoothing that has been introduced by considering merely the first five terms in the expansions in (3) does not permit a more narrow source than the one given here.

Using the average value of K, just derived, makes it possible to estimate the net flux of CO_2 between high and low latitudes due to natural sources. The distribution of these natural sources is in general agreement with the proposal of *Buch* [1939]. We find that a net transfer into the sea of approximately 2×10^{10} tons per year takes place in each hemisphere poleward of about latitude 30° and that a net release of about 4×10^{10} tons per year thus takes place in tropical regions. With a residence time for CO_2 in the mixed layer relative to the atmosphere of 5 years, corresponding to a transfer velocity of about 7×10^{-3} cm sec^{-1} in the atmospheric boundary layer [cf. *Bolin*, 1960],

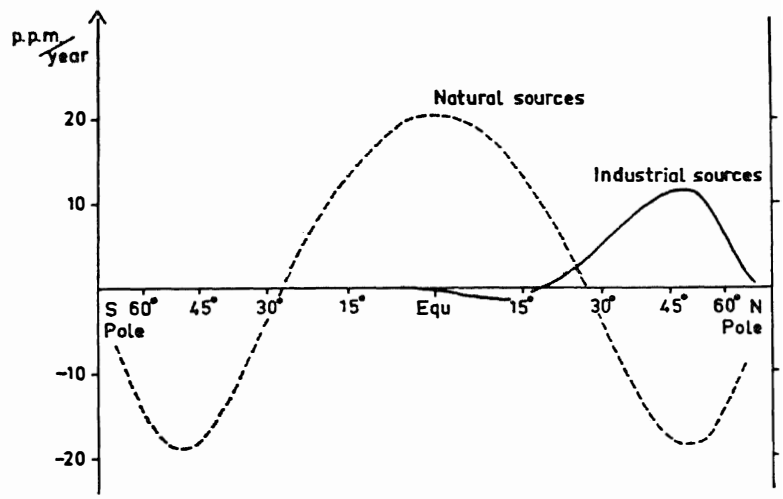

Fig. 22. The computed time-average sources and sinks of CO_2 as a function of latitude. The solid horizontal line is the latitudinal average of the natural source function. The difference, as shown by (6), is 1.6 ppm. The abscissa is in units of ppm/year averaged over the total air column.

we find that the tropical seas should have an average partial pressure of CO_2 about 50 ppm above that of the atmosphere. Presumably the exchange rate between the atmosphere and the sea changes considerably with the state of the sea surface, i.e. the wind speed, and the figure given above can only be considered as a rough average.

We next turn to an interpretation of the seasonal variations of CO_2 in the atmosphere. We subtract (2) and (1) and introduce the notations

$$q'' = q - \langle q \rangle$$

$$Q''(\mu, t) = Q(\mu, t) - [\langle Q^*(\mu) + Q^{**}(\mu) \rangle - \langle Q' + \hat{Q} \rangle \quad (9)$$

q'' expresses the seasonal variations and $Q''(\mu, t)$ gives the seasonal sources and sinks. They obviously satisfy the following differential equation:

$$\frac{\partial q''}{\partial t} = \frac{K}{a^2} \frac{\partial}{\partial \mu} \left[(1 - \mu^2) \frac{\partial q''}{\partial t} \right] + Q''(\mu, t) \quad (10)$$

We next expand q'' and $Q''(\mu, t)$ with regard to μ and t.

$$q''(\mu, t) = \sum_{n=0}^{\infty} \sum_{m=1}^{\infty} \left[q_{nm}^{(1)} \sin \frac{2\pi m t}{T} + q_{nm}^{(2)} \cos \frac{2\pi m t}{T} \right] P_n(\mu)$$

$$Q''(\mu, t) = \sum_{n=0}^{\infty} \sum_{m=1}^{\infty} \left[Q_{nm}^{(1)} \sin \frac{2\pi m t}{T} + Q_{nm}^{(2)} \cos \frac{2\pi m t}{T} \right] P_n(\mu) \quad (11)$$

where $q_{nm}^{(1)}$, $q_{nm}^{(2)}$, $Q_{nm}^{(1)}$, and $Q_{nm}^{(2)}$ are coefficients in this expansion to be determined and T is the longest period necessary to describe seasonal variations; thus $T = 1$ year. From $m = 2$, 3, etc., we obtain the higher harmonics of the seasonal variations. Our problem is to determine the source functions $Q_{nm}^{(1)}$ and $Q_{nm}^{(2)}$ that will explain the seasonal variations at all latitudes if (10) is the governing equation for the horizontal exchange. Inserting the expansions (11) into (10) and again making use of (4) we obtain the solutions

$$Q_{nm}^{(1)} = -\frac{2\pi m}{T} q_{nm}^{(2)} + \frac{K}{a^2} n(n+1) q_{nm}^{(1)}$$

$$Q_{nm}^{(2)} = \frac{2\pi m}{T} q_{nm}^{(1)} + \frac{K}{a^2} n(n+1) q_{nm}^{(2)} \quad (12)$$

The analysis of the data now consists in decomposing the seasonal curve at each latitude into harmonic oscillations with periods of 1 year, ½ year, ⅓ year, etc. The solid curves in Figure 23 show how the total amplitude of these harmonics varies with latitude. Next, each harmonic is expanded in terms of Legendre polynomials. The dashed curves in Figure 23 show how well these variations are described, including only four terms in the expansion (P_0 to P_3). The first harmonic has been smoothed in this way, but the second and third harmonics are not significantly altered. Reconstructing the seasonal variation as a function of latitude and comparing it with the observed pattern show that the essence of the pattern is obtained by considering only P_0 to P_3 and the first three harmonics in time (cf. Figures 24*a* and *b*).

Accepting the value of K given above we can now determine $Q_{nm}^{(1)}$ and $Q_{nm}^{(2)}$ from (12), and with the aid of (11) we can derive the sources and sinks as a function of time and latitude. There is, however, another independent way of determining the most likely value of the large-scale mixing coefficient that should first be discussed. Since the seasonal variations of CO_2 in the atmosphere are, in all likelihood, predominately due to land vegetation and thus originate mostly in the northern hemisphere, we can ask for the particular value of K that would give a maximum value of the ratio of the northern hemisphere source to that of the southern hemisphere. Considering, for simplicity, the first and second harmonics separately, we find the values of these ratios as a function of K as is given in Figure 25. On the basis of this result an average value of $K = 2 \times 10^{10}$ cm^2 sec^{-1} seems most likely. Figure 26 shows the amplitude of the source with a 1-year period as a function of latitude for different values of K. The figure clearly shows how values of between 2×10^{10}

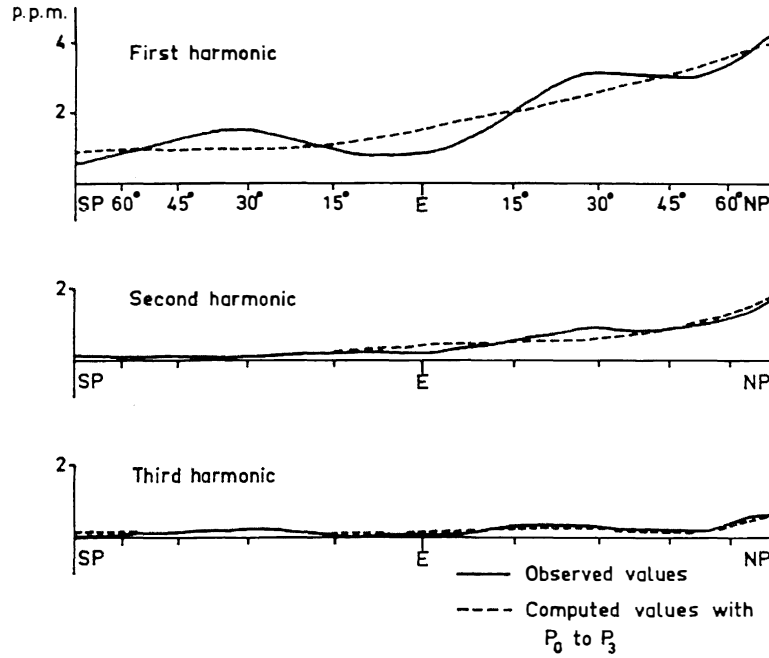

Fig. 23. Variation with latitude of the total amplitude of the first three harmonics of the seasonal curve of CO_2 (solid curves) compared with the fit obtained by the expansion in Legendre polynomials (dotted curves).

$cm^2\ sec^{-1}$ and $3 \times 10^{10}\ cm^2\ sec^{-1}$ give minimum values of the sources between latitudes 35°N and 60°S. For a computation of the intensity of these seasonal sources and sinks we shall introduce a value of $K = 2.5 \times 10^{10}\ cm^2\ sec^{-1}$. Figure 27 shows the sources and sinks thus derived as a function of season and latitude. It is seen that the essential sink in the polar regions lasts only from early June through August and that the return flow to the atmosphere has a maximum in September and October. We also see how comparatively insignificant

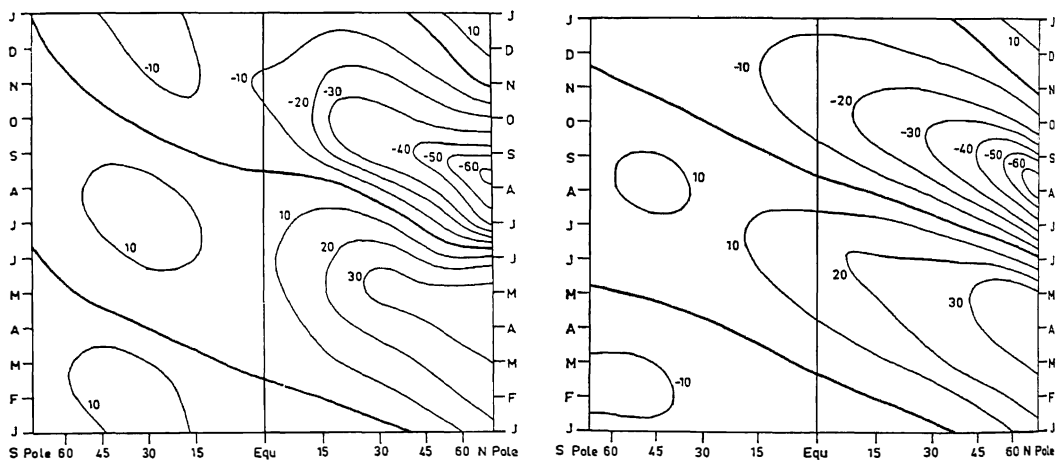

Fig. 24. Observed (*a*) and reconstructed (*b*) seasonal variation of CO_2 concentration as a function of latitude, shown as departures from the mean concentration in units of ppm × 10.

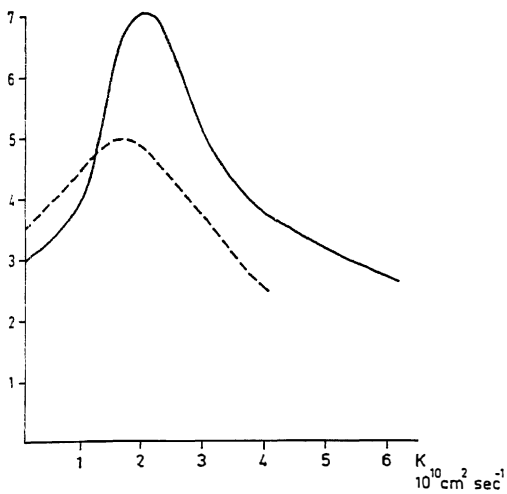

Fig. 25. Variation in the ratio of the northern hemisphere CO_2 source to that in the southern hemisphere as a function of the intensity of horizontal atmospheric mixing for the first harmonic (solid curve) and the second harmonic (dotted curve) of the seasonal variation.

the seasonal sources are in equatorial latitudes and throughout the southern hemisphere. The total sink during the few summer months in northern latitudes (north of 45°N) amounts to about 1.5×10^{10} tons, which is approximately ½ per cent of the total CO_2 content of the atmosphere. If we assume a transfer of this intensity between 500 mb and the surface of the earth and compute the eddy diffusivity in the vertical (K_z) on the basis of a concentration difference of about 2 ppm, as indicated by the data from Point Barrow and the Ptarmigan flights (Figure 28), we obtain $K_z = 3 \times 10^5$ cm^2 sec^{-1}.

Discussion. Admittedly the model used above represents a considerable simplification of the actual behavior of the atmosphere. Even for the present treatment, the data are insufficient for certain areas and for certain times of the year, and interpolations between existing observations have had to be made (cf. section on analysis of data). It is therefore quite important to establish how sensitive our results are to (*a*) the simplifications introduced by using the model of the atmosphere outlined above and (*b*) the uncertainty of the data used for the computations.

A computation of sources and sinks with equation 1 (equation 2 for steady state) essentially implies computing the second deriva-

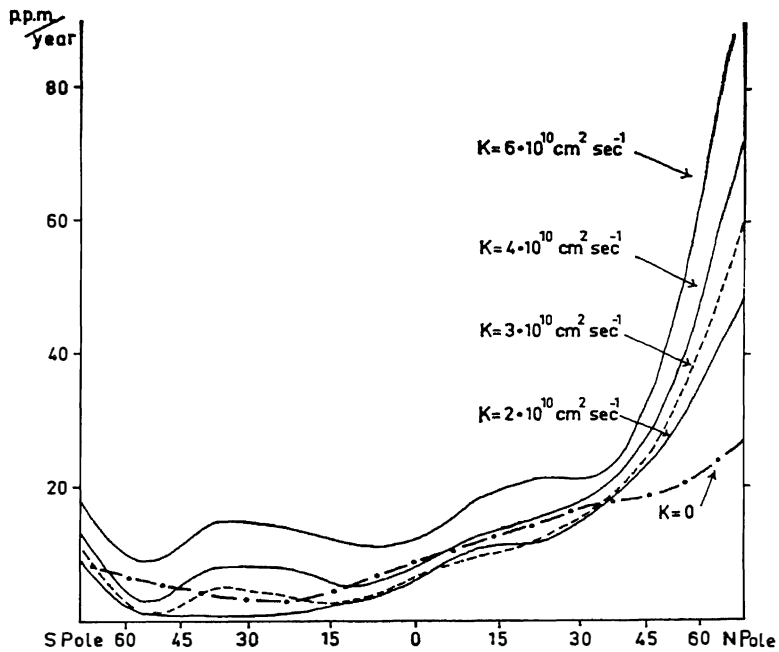

Fig. 26. Amplitude of the source for the first harmonic of the seasonal variation in CO_2 as a function of latitude for selected values of the intensity of the horizontal atmospheric mixing, K. The abscissa is in ppm/year averaged over the total air column.

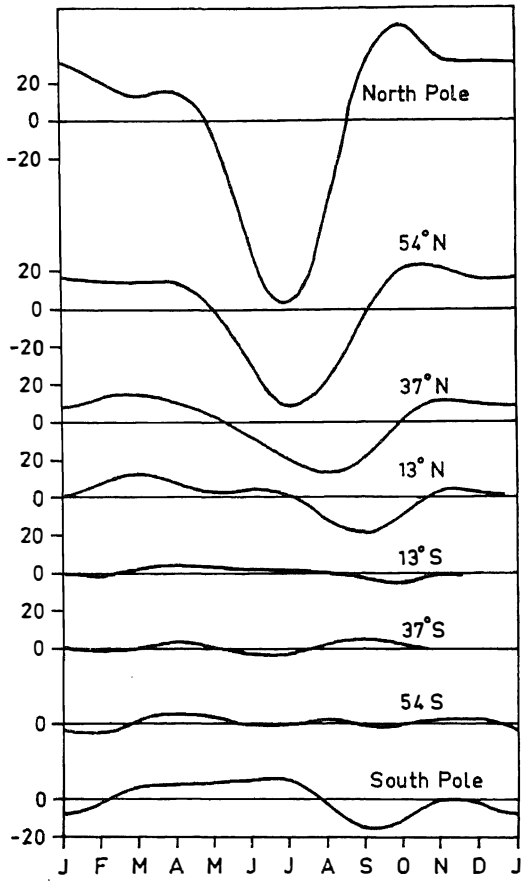

Fig. 27. Variation of the intensity of the CO_2 source with time for selected latitudes. Abscissa in units of ppm/year averaged over the total air column.

tive of the concentration as a function of latitude. One may ask how reliable such a computation is in view of the limited data. A comparison of the actually observed distribution of q as a function of latitude and the smoothed curve used for the computations also shows large variations in the second derivative, even in sign. Therefore, no details in the distribution of sources and sinks are reliable. Our results for the intensity of the natural sources in equatorial latitudes and sinks at the poles, as well as the man-made sources in middle latitudes of the northern hemisphere, are essentially based on the fact brought out by observations that the concentrations are higher around the equator than farther poleward and also higher in the northern hemisphere. In merely using the first few terms in the expansion we have considered only such features as these and have disregarded more local ones that are very uncertain.

In using (1) we have also assumed that the concentrations measured over the Pacific Ocean at a given latitude are representative for a latitude ring around the whole earth, extending through the main part of the atmosphere. In the southern hemisphere the surface is covered predominantly by oceans. The exchange rate for CO_2 between the atmosphere and the sea is comparatively slow, a characteristic exchange time being several years. Since the vertical exchange in the troposphere takes place with a characteristic time scale of about a month, the surface values should be fairly representative for such a latitude ring, except that north-south mixing is more intense at upper levels and should possibly equalize the north-south gradient more there than at the surface. This would then imply a slight vertical gradient in the tropics and polar regions corresponding to an upward transport in the tropics and a downward transport farther south, principally in agreement with the hemispheric circulation of CO_2 discussed in the preceding section. Data are, of course, too few to permit us to verify any of these statements at present, but it seems likely that the horizontal exchange rate computed in the preceding section may be somewhat lower than the average for the troposphere.

Conditions are considerably more complex in the northern hemisphere than in the southern owing to industrial combustion and the much

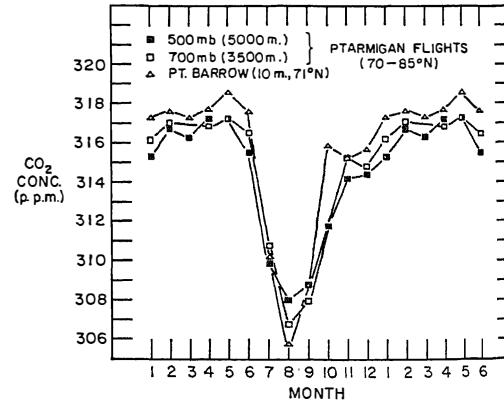

Fig. 28. Average monthly values of the concentration of atmospheric CO_2 at the surface, at 700 mb, and at 500 mb in the Arctic.

more important effect of land vegetation. Industrial combustion is concentrated in a few limited regions in middle latitudes. From these CO_2 is diffused upward and horizontally, but owing to higher winds and to more intense mixing at upper levels, CO_2 probably arrives from above at more remote places. In areas like the Pacific Ocean, therefore, somewhat higher values should prevail aloft than at the surface of the earth. One then naturally asks if this effect explains the relatively high values observed at 500 mb as compared with 700 mb and the surface between latitudes 20° to 40°N (Figure 20). Let us assume by way of illustration that the major part of all CO_2 released by combustion is redistributed over the earth through mixing at upper levels, say about 5 km, and that it is transferred to lower levels from aloft over the major part of the earth. With a vertical exchange of an intensity corresponding to $K_z \approx 10^5$ cm^2 sec^{-1}, an average difference of about 0.3 ppm between 500 mb and the surface of the earth could be constantly maintained over the whole earth, and the observed maximum of CO_2 at 500 mb in the latitude belt 20° to 40° could thus be explained. A more precise estimate than this cannot be given until a model with vertical resolution has been applied to the data (cf., for example, *Machta* [1958]).

There is one principal difference between the computed and observed seasonal variations for the southern hemisphere which should be emphasized. Comparing the two graphs (24*a* and *b*) we see that the amplitude of the computed seasonal wave decreases toward the south (except near the south polar region, where truncation of the series expansion leads to large errors), while the observed pattern shows a secondary maximum in middle latitudes in the southern hemisphere. Such a maximum, if real, must be a reflection of a seasonal source at these latitudes, and the principle of seeking the maximum of the ratio of the source intensity in the northern hemisphere to that in the southern hemisphere would not be justified in such a case. The data analysis shows, however, that very few data would be violated if the analysis was changed to exclude this secondary maximum in the seasonal wave.

According to the section on analysis of data, the gas analyzers used at field stations may yield systematically lower values than flask samples. Thus the values from the south pole could be as much as 1.0 ppm too low. Clearly the curves shown in Figures 19 and 20 would be substantially modified if this were true. The average CO_2 pressure in the two hemispheres would be almost the same in such a case. Since it is still reasonable to assume that as much of the industrial CO_2 leaves the atmosphere and goes into the oceans in the southern hemisphere as in the northern hemisphere, the intensity of the transfer from the northern to the southern hemisphere as assumed in the computations is probably no overestimate. To maintain the necessary transfer with a considerably smaller north-south gradient would require considerably more intense mixing than corresponds to $K = 3 \times 10^{10} \pm 0.5$ cm^2 sec^{-1}, the average value obtained in the present analysis. The average pole-equator difference in CO_2 pressure would not be reduced if one accepted a higher mean value at the south pole; therefore, a more intense circulation of CO_2 sources and sinks in both polar and equatorial regions would be required. Such a high value of K and of the CO_2 exchange seems very improbable both in the light of meteorological data on the large-scale horizontal exchange and from available information on atmosphere-sea exchange of CO_2 even if these data also are very uncertain. Larger values of K would also lead to a less satisfying agreement between observed and computed seasonal variations of atmospheric CO_2 concentrations, as shown in Figures 24*a* and *b*. Thus it seems likely that the south pole data are nearly correct.

The difference in the amplitude of the seasonal variations of CO_2 at various elevations above sea level as observed over the Arctic Sea is in general agreement with the computations of source intensity. Obviously, similar differences must exist in middle latitudes, and they should be detectable well into the stratosphere if the analyses were made with the present relative accuracy of 0.2 to 0.3 ppm.

Conclusion. In conclusion the following statements can be made:

1. CO_2 is an excellent tracer element for studying air circulation and mixing in the troposphere and lower stratosphere.

2. The over-all horizontal mixing of the atmosphere on a global scale corresponds to an eddy diffusivity of 3×10^{10} cm^2 sec^{-1}.

3. The north pole–equator exchange of CO_2 amounts to about 2×10^{10} tons per year.

4. The land vegetation north of about 45°N is responsible for a net CO_2 consumption of about 1.5×10^{10} tons of CO_2 during the vegetation period in the summer.

The analysis presented here could be extended considerably, and it would yield additional interesting results if more data were available. Most urgently we need: (*a*) Continuous CO_2 observations during a few years at one, preferably two, representative stations in the southern hemisphere between latitudes 20°S and 60°S; (*b*) Upper-air samples at a few levels in north polar regions, preferably also in the lower stratosphere, say at 10 or 12 km; (*c*) North-south cross sections at least once or twice a month from middle latitudes in the northern hemisphere well into the southern hemisphere, preferably along two meridians about 180° distant from each other, whereby the meridional circulation cell in the tropics as well as the representativeness of data along one meridian could be studied.

Acknowledgments. Many persons and several national agencies have contributed to the data reported here. Those mentioned earlier [*Keeling,* 1960] are collectively thanked for all additional assistance during the past two years. Additional thanks are due Messrs. Jack C. Pales, Ronald Witalis, and Lester Gillespie, of the U. S. Weather Bureau, who furnished the measurements at Mauna Loa Observatory and the South Pole Station 1960–1961 and 1961–1962, Mr. John Kelley and Dr. Paul E. Church of the University of Washington for permission to quote unpublished monthly values of the Arctic Research Laboratory at Point Barrow, Alaska, and those who obtained flask samples on board ship: Messrs. David Goheen (Limbo cruise), Richard Casey (Tethys cruise), James Coatsworth and Lee Waterman (Monsoon cruise), Christopher Harrison and Ted Rearden (Risepac cruise), Stewart Smith (Hilo cruise), and Eugene Holzapfel and Bruce Luyendyk (Proa cruise). We also thank Mr. Tom Harris of the U. S. Weather Bureau and Mr. Lee Waterman and Dr. Norris Rakestraw of the Scripps Institution of Oceanography, who handled many general aspects of the sampling program and operated the continuous gas analyzers on Downwind and Monsoon cruises.

We gratefully acknowledge the financial support of the Atmospheric Sciences and Antarctic Sciences Program of the U. S. National Science Foundation under grants Y/211/302, G-6542, G-8748, G-13657, G-17168 and of the U. S. Weather Bureau under contracts 8449, 8930, 9255, and 9473 and the support by the U. S. Office of Naval Research of the many ship operations.

The compilation of data and preparation of this paper were done at the International Institute of Meteorology in Stockholm while one of us (C.D.K.) was a fellow of the John Simon Guggenheim Memorial Foundation. We are deeply indebted to the Foundation for affording us the opportunity to collaborate at this Institute on a study which was conceived by the Institute's founder, the late Carl-Gustaf Rossby, and which was first developed here under his guidance as a contribution to the International Geophysical Year, 1957–1958.

References

Bischof, W., Variations in concentration of carbon dioxide in the free atmosphere, *Tellus, 14,* 87–90, 1962.

Bolin, B., On the exchange of carbon dioxide between the atmosphere and the sea, *Tellus, 12,* 274–281, 1960.

Buch, K., Beobachtungen über das Kohlensäuregleichgewicht und über den Kohlensäureaustausch zwischen Atmosphäre und Meer im Nordatlantischen Ozean, *Acta Acad. Aboensis, Math. Phys., 11*(9), 1–32, 1939.

Keeling, C. D., The concentration and isotopic abundance of carbon dioxide in the atmosphere, *Tellus, 12,* 200–203, 1960.

Machta, L., Global scale dispersion by the atmosphere, *Proc. 2nd U. N. Intern. Conf. Peaceful Uses At. Energy, Geneva, 1958,* Session D-19, pp. 519–525, 1958.

Pales, J. C., and C. D. Keeling, The concentration of atmospheric carbon dioxide at Mauna Loa Observatory, Hawaii, submitted to *J. Geophys. Res.,* 1963.

(Manuscript received January 25, 1963; revised March 14, 1963.)